IRJSE International Research Journal of Science & Engineering
Int. Res. J. of Science & Engineering, 2018; Special Issue A5 : 53-56
ISSN: 2322-0015
SJIF Impact Factor 2016: 6.68
UGC Approved Journal No. 63628
RESEARCH ARTICLE **OPEN ACCESS**

Sol-Gel Synthesized $Y_{3-x}Bi_xAl_{0.5}Fe_{4.5}O_{12}$ nanoparticles: Structural and electrical investigations

[1]Borade RB,[2]Kadam SB, [3]Shinde Vishnu, [4]Alone ST, [5]Dhale LA, [1]Gaikwad AS and [1*]Kadam AB

[1]Physics Department, Jawahar Mahavidyalaya, Andur, Dist. Osmanabad (M.S.) India
[2]Physics Department, L.B.S. College, Partur, Dist. Jalna (M.S.) India
[3]Chemistry Department, Shivaji College, Omerga, Dist. Osmanabad (M.S.) India
[4]Physics Department, Rajasrshi Shahu College, Pathri, Dist. Aurangabad (M.S.) India
[5]Chemistry Department, Shrikrishna College, Gunjoti, Dist. Osmanabad (M.S.) India
[*]Corresponding Author: drabkadam@gmail.com

Manuscript Details

Available online on http://www.irjse.in
ISSN: 2322-0015

Editor: Dr. Arvind Chavhan

Cite this article as:
Borade RB, Kadam SB, Shinde Vishnu, Alone ST, Dhale LA, Gaikwad AS and Kadam AB. Sol-Gel Synthesized $Y_{3-x}Bi_xAl_{0.5}Fe_{4.5}O_{12}$ nanoparticles: Structural and electrical investigations, *Int. Res. Journal of Science & Engineering*, 2018; Special Issue A5: 53-56.

ABSTRACT

Sol-gel auto-combustion synthesized $Y_{3-x}Bi_xAl_{0.5}Fe_{4.5}O_{12}$ nanoparticle powders were finally sintered at 1150 °C for 10 h, on the basis of DTA/TG analysis. The crystalline structure was investigated by using X-ray diffractograms. The XRD analysis confirms a single phase garnet structure for $x \geq 1.0$. The DC resistivity as a function of temperature was studied using the two-probe method and it gives the decreasing trend with increasing temperature for all samples.

Key words Sol-Gel Synthesis, garnet, D.C. resistivity

INTRODUCTION

Pure and substituted yttrium iron garnet (YIG) is an important substance used in magneto-optical and microwave application [1, 2]. Yttrium iron garnet useful for microwave devices like phase shifters, circulators oscillators and optical isolators because they have comparatively low dielectric loss behavior, narrow line width at GHz frequencies and low magnetization [3,4]. YIG with chemical formula ($Y_3Fe_5O_{12}$) has unique electromagnetic, thermal and

mechanical properties [5]. Due to low propagation loss and large magneto-optic effect, trivalent ion substituted YIG is superior candidate substances for the devices with higher quality [6, 7]. The physical properties of YIG can be changed by substituting various elements Dy^{3+}, Ce^{3+}, Er^{3+}, Tb^{3+} or Bi^{3+} with Y^{3+} ion [8, 9]. Many workers have studied the structural, magnetic and electrical properties of pure and doped YIG [10-13].

However, there is no work reported on the substitution of Bi^{3+} in the Al-doped yttrium iron garnet nanoparticles. Therefore, we have prepared $Y_{3-x}Bi_xAl_{0.5}Fe_{4.5}O_{12}$ (x = 0.0, 0.5, 1.0) powders using sol-gel technique. This paper is focused on the effect of Bi^{3+}substitution in Al-doped YIG on structural and electrical properties.

METHODOLOGY

The starting solution containing nitrates (98.5 % pure) was prepared by dissolving and mixing the stoichiometric quantity of the nitrates in 100 ml distilled water. Citric acid was then added to the prepared aqueous solutions which work as a chelating agent in solution. This mixture was constantly stirred with the help of magnetic agitator and vaporized by heating at around 80-90 ^{0}C till the precipitation. These were heated at around 150^{0}C for the ignition of the precipitates and converted into ash. The pellets of 1 gm powder were formed by pressing 5-ton pressure having 10 mm diameter and around 3-4 mm thickness. The phase identification and crystalline structures powders were investigated by X-ray diffractometer (XRD) with Cu-k_α radiation λ=1.5404 (Ultima IV Rigaku). DC resistivity of samples was carried out as a function of temperature by using two probe experimental set-ups using silver paste contact.

RESULTS AND DISCUSSIONS

In order to gain more insight into the phase evolution, phase transformation and to determine the possible temperature of decomposition of as-combusted powders was studied using DTA/TG measurements for the composition $Y_{3-x}Bi_xAl_{0.5}Fe_{4.5}O_{12}$ (x = 1.0) in air. The heating rate was 10 °C/min with temperature range 20 to 1185 °C. The Combined DTA/TG analysis curves of a $Y_2Bi_1Al_{0.5}Fe_{4.5}O_{12}$ composition is shown in Fig. 1. The TG data of as-combusted $Y_2Bi_1Al_{0.5}Fe_{4.5}O_{12}$ powder prepared by sol-gel auto-combustion classified in the three steps upto the 1185 °C. The room temperature to 250 °C is attributed to the vaporization of absorbed water. In second step 250 to 607 °C is related to the residual organic matter and citric acid. In third step, unreacted metal nitrate is oxidized above the 607 °C temperature. TGA curve indicates the total weight loss around 1185 °C is 50%. The presence of an exothermic peak on the DTA curve at about 470^{o}C indicates the burning of organic derivatives. The decomposition has completed around 1100 °C, therefore we have selected 1150 °C as annealing temperature for $Y_{3-x}Bi_xAl_{0.5}Fe_{4.5}O_{12}$ (x = 0.0, 0.5, 1.0) samples. The phase formation of YIG around at this temperature is confirmed by XRD analysis.

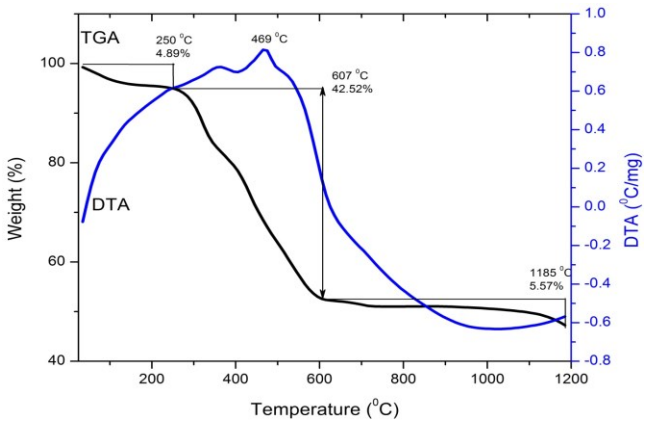

Fig. 1: TG-DTA plot of as –prepard sample $Y_{3-x}Bi_xAl_{0.5}Fe_{4.5}O_{12}$ (x = 1.0) composition

The X-ray diffraction patterns of $Y_{3-x}Bi_xAl_{0.5}Fe_{4.5}O_{12}$ (x = 0.0, 0.5, 1.0) sintered at 1150^{0}C for 10 h is shown in Fig. 2. The crystalline planes (400), (420), (332), (422), (521), (532), (444), (640), (642), (800), (840), (842) and (644) well matches with standard JCPDS #43-0507 for pure YIG. The XRD patterns obtained, exhibit formation of single phase cubic YIG. The garnet phase is observed predominately whereas a weak Bi_2O_3 phase along with

another secondary phase.

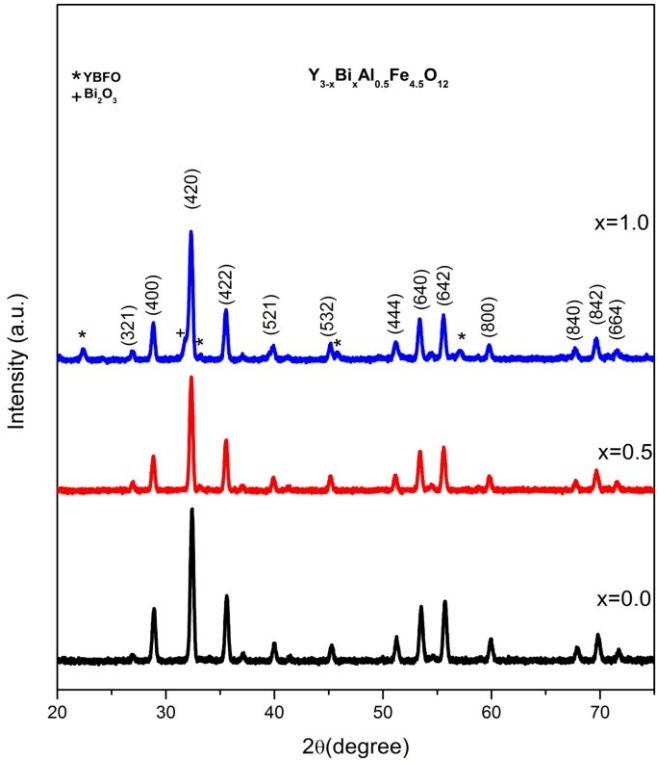

Fig. 2: XRD patterns of $Y_{3-x}Bi_xAl_{0.5}Fe_{4.5}O_{12}$.

The most intense peak (420) of undoped $Y_3Al_{0.5}Fe_{4.5}O_{12}$ (x = 0.0) is located at 2θ = 32.41^0, it shifts slightly towards lower diffraction angles as Bi^{3+} content increases from x = 0.0 to x = 1.0**.** The lattice parameter (a) was computed with the help of Bragg's equation

$$a = \sqrt{\frac{\lambda^2}{4\sin^2\theta}\left(h^2+k^2+l^2\right)} \qquad (1)$$

The lattice parameter of sample increases by increasing the Bi^{3+} composition and diffraction lines shift towards the lower diffraction angles. This is because of replacement of smaller Y^{3+} (0.9 Å) ion by the larger Bi^{3+} (1.17 Å) which gives the enlargement of lattice parameter. Table 1 shows the variation of lattice parameter with increasing Bi^{3+} concentration. The lattice parameter increases from 12.35 Å to 12.39 Å for x is increased from 0 to 1.0 which exhibits the incorporation of Bi^{3+} into the lattice of YIG. This behavior was also reported for $Y_{3-x}Bi_xFe_5O_{12}$ nanoparticles [14]. The values are between 12.35 Å to 12.39 Å, well-matched with standard JCPDS data. The grain size of the nano-particles was computed from the most intense peak (420) of XRD data. X-ray density was calculated by using the XRD data. The calculated values X-ray density are summarized in table 1. The X-ray density increases with increasing bismuth composition. This is due to the increase in molecular weight which is proportional to the X-ray density.

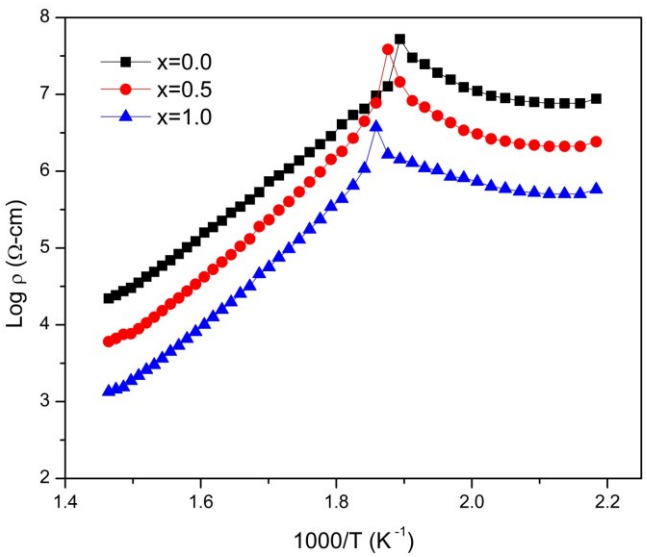

Fig. 3: Variation of log ρ versus 1000/T for $Y_{3-x}Bi_xAl_{0.5}Fe_{4.5}O_{12}$

The variation of DC resistivity with temperature in garnet samples is shown in Fig.3. The measured DC resistivity decreases with increasing temperature for all samples which indicates that all the prepared samples are semiconductors. The observed DC electrical resistivity decreases with increasing temperature due to the increase of the drift mobility of charge carriers. DC resistivity decreases with the substitution of Bi^{3+} ions concentration in YIG which attribute the increase in conductivity due to the electron hopping between the charge carriers. The garnet system exhibits an exponential dependence of DC electrical resistivity with temperature. The resistivity of the garnet shows Arrhenius type [15-16] temperature dependence and is given by the equation $\rho = \rho_0 e^{\left(\frac{-E_g}{KT}\right)}$, where Eg is the activation energy and k is Boltzmann constant.

Table 1: Lattice parameter 'a', X-ray density 'dx' and transition temperature T_C for $Y_{3-x}Bi_xAl_{0.5}Fe_{4.5}O_{12}$

'x'	'a' Å	dx (gm/cc)	T_C (K)
0.0	12.35	5.11	527
0.5	12.37	5.50	533
1.0	12.39	5.89	537

CONCLUSION

Nanocrystalline $Y_{3-x}Bi_xAl_{0.5}Fe_{4.5}O_{12}$ garnet nanoparticles were successfully synthesized at 1150 °C by sol-gel auto-combustion method. The garnet phase is observed predominately in the case of x = 0.0, 0.5 and 1.0. The lattice parameter increases with the composition increase of Bi concentration. The DC resistivity of the samples are found to be decreased with increasing the temperature and it decreases with increasing Bi^{2+} ion substitution for a fixed Al^{3+} ion concentration. The the samples with $x \geq 1.0$ exhibits excellent properties which has potential application for microwave and magneto-optical devices.

REFERENCES

1. Garskaite E, Gibson K, Leleckaite A, Glaser J, Niznansky D, Kareiva A, Meyer HJ. Chemical physics, 323, 2006,204-210
2. Higuchi S, Takekawa S, Kitamura K. Japanese journal of applied physics, 38, 1999, 4122.
3. Harris VG, Geiler A, Chen Y, Yoon SD, Wu M, Yang A, Chen Z, He P, Parimi PV, Zuo X. Journal of Magnetism and Magnetic Materials, 321, 2009, 2035-2047
4. Adam JD, Davis LE, Dionne GF, Schloemann EF, Stitzer SN. IEEE Transactions on Microwave Theory and Techniques, 50, 2002, 721-737.
5. Kareiva A. Materials Science, 17, 2011, 428-436
6. Xu H, Yang H, Xu W, Feng S. Journal of Materials processing technology, 197, 2008, 296.
7. Sekhar MC, Hwang JY, Ferrera M, Linzon Y, Razzari L, Harnagea C, Zaezjev M, Pignolet A, Morandotti R. Applied Physics Letters, 94, 2009,181916.
8. Cheng Z, Yang H, Cui Y, Yu L, Zhao X, Feng S. J. Magn. Magn. Mater., 308, 2007, 5-9.
9. Shaiboub R, Ibrahim NBY, Abdullah M, Abdulhade F. J. Nanomater, 2012, 2012) 2.
10. Arsad A, Ibrahim N. Journal of Magnetism and Magnetic Materials, 410, 2016, 128-136
11. Arun T, Vairavel M, Raj SG, Joseyphus RJ. Ceramics International, 38, 2012, 2369-2373
12. Aldbea FW, Ibrahim N, Abdullah MH, Shaiboub RE. J. Sol-Gel Sci. Tech., 62, 2012, 483.
13. Zhao H, Zhou J, Bai Y, Gui Z, Li L. J. Magn. Magn. Mater, 280, 2004, 208-213.
14. Matsumoto K, Yamaguchi K, Fujii T, Ueno A. Journal of Applied Physics, 69,1991, 5918.
15. Klages CP, Tolksdorf W, Kumpat G. Journal of Crystal Growth, 65,1983, 556.
16. Modi KB, Sharma PU. Radiation Effects and Defects in Solids, 168, 2013, 967.